INTERNATIONAL JOURNAL OF LATEST TECHNOLOGY IN ENGINEERING, MANAGEMENT & APPLIED SCIENCE (IJLTEMAS)

ISSN 2278-2540 | DOI: 10.51583/IJLTEMAS | Volume XIV, Issue X, October 2025

Magnetohydrodynamic Unsteady Convective Heat and Mass Transfer along a Semi-Infinite Permeable Vertical Plate with Heat Absorption

Sindhu

Department of Mathematics, Dr. N.G.P Arts and Science College, Coimbatore 641048, Tamil Nadu, India

DOI: https://doi.org/10.51583/IJLTEMAS.2025.1410000048

Abstract: The study investigates the unsteady, two-dimensional, laminar boundary-layer flow of a viscous, incompressible, electrically conducting, and heat-absorbing fluid past a semi-infinite vertical permeable moving plate. The flow is influenced by a uniform transverse magnetic field, along with thermal and concentration buoyancy effects. The plate moves at a constant velocity in the direction of the fluid motion, while the free-stream velocity follows an exponentially increasing small perturbation law. Time-dependent wall suction is applied at the permeable surface. The dimensionless governing equations are analytically solved using two-term harmonic and non-harmonic functions. The obtained solutions are shown to reduce to previously reported results under special limiting conditions. Numerical evaluation of the analytical expressions is carried out, and graphical illustrations of the velocity, temperature, and concentration distributions within the boundary layer are provided. Additionally, tabulated results for the skin-friction coefficient, Nusselt number, and Sherwood number are presented and discussed.

Keywords: Free convection, chemical reaction, MHD, suction, skin friction.

I. Introduction

Free convection takes place when a fluid's temperature differences create density changes, generating buoyancy forces that move the fluid. Research on heat and mass transfer in magnetohydrodynamic (MHD) free-convection flows with chemical reactions and thermal radiation along a vertical plate has grown steadily in recent years. Precise understanding of this type of convective heat transfer is crucial for many engineering and scientific areas. Examples include thermal insulation, drying of porous materials, heat exchangers, steam pipelines, water heaters, refrigeration systems, and electrical equipment. It is also important in industrial, geophysical, and astrophysical settings such as polymer and ceramic manufacturing, packed-bed catalytic reactors, food processing, nuclear reactor cooling, enhanced oil recovery, underground energy transport, magnetized plasma flows, high-speed plasma winds, cosmic jets, and stellar phenomena. In high-temperature operations—such as glass making, furnace design, propulsion systems, plasma research, and spacecraft re-entry—the contribution of thermal radiation becomes especially significant. Wang et. al [1] investigated the free convection heat transfer in thermal imaging processes. The free-convection equations were analytically solved for both purely steady-state and purely unsteady conditions. According to Viswanathan, S. H., *et al.* [2], the influence of human body shape on free-convection heat transfer was investigated. They discovered that the free-convection heat-transfer coefficient remains unaffected by a person's sex or height, but it declines slightly as the body-mass index (BMI) rises. Wang, L. et al. [3] analysed free convection heat transfer in thermal imaging processes. They finally concluded the calculation of convective heat transfer in thermal imaging experiments using step-, square-, and flash-heating excitations. Chamkha [4] has examined hydromagnetic natural convection from an isothermal inclined surface in contact with a thermally stratified porous medium.

Recent investigations on magnetohydrodynamic (MHD) flow and heat transfer have significantly broadened the understanding of combined thermal and magnetic effects in various engineering systems. Wang et al. [7] studied free convection heat transfer in thermal imaging processes and demonstrated that the mode of heating—such as step, square, or flash excitations—has a considerable influence on the rate of convective heat transfer. Viswanathan et al. [8] examined the impact of human body geometry on free convection heat transfer and found that while the heat-transfer coefficient is largely independent of sex or height, it slightly

decreases with increasing body mass index (BMI). In addition, Chamkha [9] and other researchers have analysed the influence of magnetic fields and heat absorption on unsteady convective flows over vertical permeable plates embedded in porous media. These studies collectively emphasize how the interaction between magnetic strength, chemical reaction, and heat absorption affects velocity, temperature, and concentration distributions in electrically conducting fluids. Such findings have laid a strong foundation for the present investigation, highlighting the importance of coupling MHD effects with thermal and solutal convection phenomena for both theoretical understanding and practical applications.

Mathematical Formulation:

This study examines the time-dependent, 2D-flow of a laminar, viscous, A constant-density fluid, electrically conducting, and heat-absorbing fluid past a semi-infinite vertical permeable plate that is moving and embedded within a uniform porous medium. The system is influenced by a uniform transverse magnetic field and experiences thermal and concentration buoyancy effects. The governing equations for this flow are derived from the conservation laws of mass, linear momentum, energy, and species concentration. Based on the assumptions outlined, these equations can be expressed in a Cartesian coordinate system as follows:

ISSN 2278-2540 | DOI: 10.51583/IJLTEMAS | Volume XIV, Issue X, October 2025

$$\frac{\partial \vartheta^*}{\partial y^*} = 0 \ldots\ldots (1)$$

$$\frac{\partial u^*}{\partial t^*} + \vartheta^* \frac{\partial u^*}{\partial y^*} = -\frac{1}{\rho}\frac{\partial p^*}{\partial x^*} + \vartheta^* \frac{\partial^2 u^*}{\partial y^{*2}} + g\beta_T(T - T_\infty) + g\beta_C(T - T_\infty) - \vartheta^* \frac{u^*}{k^*} - \frac{\sigma}{\rho} B_0^2 u^* \ldots\ldots (2)$$

$$\frac{\partial T}{\partial t^*} + \vartheta^* \frac{\partial T^*}{\partial y^*} + \alpha \frac{\partial^2 T}{\partial y^{*2}} - \frac{Q_0}{\rho C_P}(T - T_\infty) \ldots\ldots (3)$$

$$\frac{\partial C}{\partial x^*} + \vartheta^* \frac{\partial C}{\partial y^*} + \alpha \frac{\partial^2 C}{\partial y^{*2}} - K(C - C_\infty) \ldots\ldots (4)$$

Here, x^*, y^*, and t^*represent the dimensional distances along and perpendicular to the plate, and dimensional time, respectively. U^* and V^* denote the components of dimensional velocity in the x^* and y^* directions, respectively. The fluid density is ρ and ν is the kinematic viscosity, $c_p$is the specific heat at constant pressure, σ is the electrical conductivity of the fluid, B_0 is the magnetic field induction, and K^* is the permeability of the porous medium. T stands for dimensional temperature, Q0 is the dimensional heat absorption coefficient, C is the dimensional concentration, α is the thermal diffusivity, D is the mass diffusivity, g is the acceleration due to gravity, β_T and β_C and are the thermal and concentration expansion coefficients, respectively. Magnetic and viscous dissipation effects are neglected in this study.

Based on these assumptions, the boundary conditions for the velocity, temperature, and concentration fields are defined as follows:

$u^* = u^*_{p,}$ T=$T_W + \varepsilon(T_W - T_\infty)e^{n^* t^*}$, C=$C_W + \varepsilon(C_W - C_\infty)e^{n^* t^*}$ $at\ y^* = 0$……(5)

$u^* \to U^*_\infty = U_0(1 + \varepsilon e^{n^* t^*})$, T→$T_\infty$, C→$C_\infty$, as $y^* \to \infty$……(6)

Here, $u^*_{p,}$ and C_W, T_W denote the dimensional wall velocity, concentration, and temperature, respectively, while U^*_∞ and C_∞, T_∞ represent the corresponding free-stream dimensional velocity, concentration, and temperature. The quantities U_0 and n^* are constants. Assuming that it takes the following exponential form:

$$\vartheta^* = -V_0(1 + \varepsilon A e^{n^* t^*}) \ldots\ldots (7)$$

A is a positive real constant; ε and εA are both small values less than one and V_0represents the suction-velocity scale, which is a positive constant greater than zero. Outside the boundary layer, Eq (2) give

$$-\frac{1}{\rho}\frac{d\rho^*}{dx^*} = \frac{dU_\infty}{dt^*} + \frac{\vartheta}{K^*}U^*_\infty + \frac{\sigma}{\rho}B_0^2 U^*_\infty \ldots\ldots (8)$$

To simplify the governing equations, we introduce the following set of dimensionless variables.

u=$\frac{u^*}{U_0}$, v=$\frac{v^*}{v_0}$, $\eta = \frac{v_0 y^*}{\vartheta}$, U_∞=$\frac{U_\infty}{U_0}$, U_∞=$\frac{u^*_p}{U_0}$, t=$\frac{t^* V_0^2}{\vartheta}$,θ=$\frac{T - T_\infty}{T_W - T_\infty}$, ϕ=$\frac{C - C_\infty}{C_W - C_\infty}$, n=$\frac{\nu n^*}{V_0^2}$, K=$\frac{V_0^2 K^*}{\nu^2}$, Pr=$\frac{\nu \rho c_\rho}{k}$=$\frac{\nu}{\alpha}$,

sc =$\frac{\vartheta}{D}$, M=$\frac{\sigma B_0^2 \nu}{\rho v_0^2}$, G_T=$\frac{\nu \beta_T g(T_W - T_\infty)}{U_0 V_0^2}$, , G_C=$\frac{\nu \beta_C g(C_W - C_\infty)}{U_0 V_0^2}$,ϕ=$\frac{\nu Q_0}{\rho C_P V_0^2}$, Kr=$\frac{k\nu}{V_0^2}$……..(9)

Using Eqs. (7)– (9), the set of Eqs. (2)– (4) can be transformed into the following dimensionless form:

$$\frac{\partial u}{\partial t} - (1 + \epsilon A e^{nt})\frac{\partial u}{\partial \eta} = \frac{dU_\infty}{dt} + \frac{\partial^2 u}{\partial \eta^2} + G_T\theta + G_c C + N(U_\infty - u) \ldots\ldots (10)$$

$$\frac{\partial \theta}{\partial t} - (1 + \epsilon A e^{nt})\frac{\partial \theta}{\partial \eta} = \frac{1}{Pr}\frac{\partial^2 \theta}{\partial \eta^2} - \theta\phi \ldots\ldots (11)$$

$$\frac{\partial c}{\partial t} - (1 + \epsilon A e^{nt})\frac{\partial c}{\partial \eta} = \frac{1}{Sc}\frac{\partial^2 C}{\partial \eta^2} - KrC \ldots\ldots (12)$$

Here N=(M+$\frac{1}{K}$) and G_T, G_c, Pr, ϕ and Sc represent the thermal Grashof number, solutal Grashof number, Prandtl number, dimensionless heat absorption coefficient, and Schmidt number, respectively.

The boundary conditions given in (5) and (6) can be expressed in the following dimensionless form:

$u = U_{p,}$ θ=1+ϵe^{nt}, c=1+ϵe^{nt}, at η= 0 ……(13)

u→ $U_{\infty,}$ θ→ 0, C→ 0 as η→ ∞…… (14)

ISSN 2278-2540 | DOI: 10.51583/IJLTEMAS | Volume XIV, Issue X, October 2025

Nomenclature	
A	Suction velocity parameter
B_0	Magnetic induction
C	Concentration
c_p	Specific heat at constant pressure
C	Dimensionless concentration
c_f	Skin friction coefficient
D	Mass diffusion coefficient
G_C	Solutal Grashof number
G_T	Thermal Grashof number
G	Acceleration due to gravity
K	Permeability of the porous medium
K	Thermal conductivity
M	Magnetic field parameter
N	Dimensionless exponential index
N	Dimensionless exponential index
Nu	Nusselt number
Pr	Prandtl number
Q_0	Heat absorption coefficient
Re_x	Local Reynolds number
Sc	Schmidt number
Sh	Sherwood Number
T	Temperature
T	Dimensionless time
U_0	Scale of free stream velocity
u, v	Component of velocity along and perpendicular to the plate, respectively.
V_0	Scale of suction velocity
x, y	Distance along the perpendicular to the plate, respectively
Greek symbols	
A	Fluid thermal diffusivity
β_c	Coefficient of volumetric concentration expansion
β_T	Coefficient pf Volumetric thermal expansion
ϵ	Scalar constant
H	Dimensionless normal distance
Φ	Dimensionless heat absorption coefficient
Σ	Fluid electrical conductivity
P	Fluid density

ISSN 2278-2540 | DOI: 10.51583/IJLTEMAS | Volume XIV, Issue X, October 2025

M	Fluid dynamic viscosity
N	Fluid kinematic viscosity
T	Friction coefficient
Θ	Dimensionless temperature

Solution of the Problem

Equations (10)– (12) constitute a system of partial differential equations that do not admit a closed-form solution. Nevertheless, they can be transformed into a set of dimensionless ordinary differential equations that are solvable analytically. This transformation is achieved by expressing the velocity, temperature, and concentration as follows:

$U=f_0(\eta)+f_1(\eta)\epsilon e^{nt}+o(\epsilon^2)+\cdots$ ……(15)

$\theta=g_0(\eta)+g_1(\eta)\epsilon e^{nt}+o(\epsilon^2)+\cdots$ ……(16)

$C=h_0(\eta)+h_1(\eta)\epsilon e^{nt}+o(\epsilon^2)+\cdots$ ……(17)

By substituting Eqs. (15)– (17) into Eqs. (10)– (12), and then matching the harmonic and non-harmonic components while neglecting higher-order terms of $o(\varepsilon^2)$, we arrive at the following sets of equations corresponding to (f_0, g_0, h_0) and (f_1, g_1, h_1).

$f_0''+f_0'-Nf_0=-N-G_Tg_0-G_Ch_0$ ……(18)

$f_1''+f_1'-(N+n)f_1=-Af_0'-G_Tg_1-G_Ch_1-(N+n)$ ……(19)

$g_0''+Prg_0'-Pr\phi g_0=0$……(20)

$g_1''+Prg_1'-Pr\phi g_1nc-Pr\phi g_1=-APrg_0'$ ……(21)

$h_0''+Sch_0'-ScKrh_0=0$……(22)

$h_1''+Sch_1-Sc(Kr+n)h_1=-ASch_0'$……(23)

Here, a prime indicates differentiation with respect to η. The associated boundary conditions can be expressed as follows:

$f_0=U_P, f_1=0, g_0=1, g_1=1, h_0=1, h_1=1$ at η=0…….. (24)

$f_0=1, f_1=1, g_0\to 0, g_1\to 0, h_0\to 0, h_1\to 0$ as $\eta\to\infty$…… (25)

Without presenting the intermediate steps, the solutions of Eqs. (18)– (23), subject to the boundary conditions (24) and (25), are found to be:

$f_0=1+C_2e^{-\lambda_1\eta}+A_3e^{-m_3\eta}+A_4e^{-m_1\eta}$ ……(26)

$f_1=1+C_4e^{-\lambda_3\eta}+A_5e^{\eta}+A_4e^{-m_1\eta}$ ……(27)

$g_0=e^{-m_3\eta}$ ……(28)

$g_1=e^{-m_7\eta}+A_2(e^{-m_5\eta}-e^{-m_7\eta})$……(29)

$h_0=e^{-m_1\eta}$…… (30)

$h_1=e^{-m_3\eta}+A_1(e^{-m_1\eta}-e^{-m_3\eta})$…….. (31)

Based on the above solutions, the boundary layer profiles for velocity, temperature, and concentration can be expressed as

$u(\eta,t)=(1+C_2e^{-\lambda_1\eta}+A_3e^{-m_3\eta}+A_4e^{-m_1\eta})+\epsilon e^{nt}(1+C_4e^{-\lambda_3\eta}+A_5e^{-\lambda_1\eta}+A_6e^{-m_5\eta}+A_7e^{-m_1\eta}+A_8e^{-m_7\eta}+A_9e^{-m_3\eta})$……(32)

$\theta(\eta,t)=(e^{-m_5\eta})+\epsilon e^{nt}A_2(e^{-m_5\eta}-e^{-m_7\eta})$…… … (33)

$C(\eta,t)=(e^{-m_1\eta})+\epsilon e^{nt}A_2(e^{-m_1\eta}-e^{-m_3\eta})$…… (34)

In boundary-layer flow analysis, the skin-friction coefficient, Nusselt number, and Sherwood number serve as significant physical parameters. They are defined and calculated in the following manner:

$C_f=\frac{\partial u}{\partial\eta}=(-C_2\lambda_1-m_5A_3-A_4m_1)+\epsilon e^{nt}(-\lambda_3C_4-\lambda_1A_5-m_5A_6-m_1A_7-m_7A_8-m_3A_9)$

$Nu=NuRe^{-1}=\frac{\partial\theta}{\partial\eta}=-m_5+\epsilon e^{nt}(-m_7-m_5A_2+m_7A_2)$

ISSN 2278-2540 | DOI: 10.51583/IJLTEMAS | Volume XIV, Issue X, October 2025

Sh=ShRe^{-1}=-m_1+ $\epsilon e^{nt}(-m_3 - m_1A_1 + m_3A_1)$

Here, $Re^{-1} = \frac{V_0 x}{\nu}$represents the local Reynolds number. It is worth noting that when the effects of concentration buoyancy and heat absorption are neglected, the obtained flow and heat transfer solutions agree with the earlier results presented by Chamka [5].

Table 1 Effects of on Gr_c on $C_f, \frac{Nu}{Re_x}, and\ \frac{Sh}{Re_x}$.

G_c	c_f	$\frac{Nu}{Re_x}$	$\frac{Sh}{Re_x}$
0	2.7200	-1.7167	-0.8098
1	3.2772	-1.7167	-0.8098
2	3.8343	-1.7167	-0.8098
3	4.3915	-1.7167	-0.8098
4	4.9487	-1.7167	-0.8098

Table 2 Effects of on ϕ on $C_f, \frac{Nu}{Re_x}, and\ \frac{Sh}{Re_x}$.

G_c	c_f	$\frac{Nu}{Re_x}$	$\frac{Sh}{Re_x}$
0	3.4595	-1.0699	-0.8098
1	3.2772	-1.7167	-0.8098
2	3.1933	-2.1193	-0.8098
3	3.1378	-2.4388	-0.8098

Table 3 Effects of on Sc on $C_f, \frac{Nu}{Re_x}, and\ \frac{Sh}{Re_x}$.

Sc	c_f	$\frac{Nu}{Re_x}$	$\frac{Sh}{Re_x}$
0.16	3.4328	-1.7167	-0.2231
0.6	3.2772	-1.7167	-0.8098
1	3.1847	-1.7167	-1.3425
2	3.0481	-1.7167	-2.6741

II. Result and Discussion

The table results are presented to demonstrate how the chemical reaction parameter Kr, the Schmidt number Sc, the heat absorption coefficient α, and the magnetic field parameter M affect the velocity, temperature, and concentration profiles. In this analysis, the remaining physical parameters are held constant with the following values: A=0.5, β=0.2, Gt=2, Gc=1, M=0, Sc=0.6, k=0.5, α=1, oscillation frequency n=0.1, free stream velocity scale up=0.5, Prandtl number Pr=0.7, and time t=0. Figures 1 and 2 illustrate the velocity and concentration profiles, respectively. It is observed that both velocity and concentration decrease as the chemical reaction parameter *Kr* increases. Additionally, the streamwise velocity magnitude diminishes, and the inflection point of the velocity profile shifts farther from the surface. **When the chemical reaction parameter (Kr) increases, the rate of destructive chemical reaction within the fluid becomes stronger. This means that the concentration of the diffusing species (the solute) near the plate is reduced because more of it is being consumed by the chemical reaction.**

The chemical reaction parameter {Kr} models the consumption or generation of chemical species within the fluid, which is linked to flow through density changes (buoyancy) and is critical for process efficiency.

- **Chemical Reactors and Catalysis:** Optimizing the design of heterogeneous and homogeneous **chemical reactors**. By understanding how the reaction rate Kr affects the concentration distribution, engineers can maximize product yield and minimize unwanted side-reactions.

ISSN 2278-2540 | DOI: 10.51583/IJLTEMAS | Volume XIV, Issue X, October 2025

- **Pollution Control (Air/Water Quality):** Modelling the dispersion and decay of pollutants in the atmosphere or waterways. The Kr parameter represents the rate at which pollutants are chemically degraded or neutralized.
- **Biomedical Drug Delivery:** Analysing the release and absorption of drugs in biological fluids. The Kr factor simulates the rate at which the drug reacts with the tissue or fluid, which is essential for determining effective dosage and release kinetics.
- **Combustion Science:** The reaction kinetics Kr are paramount in modelling flame propagation and combustion efficiency, helping design more efficient engines and burners by controlling the mixing and consumption rates of fuel/oxidizer.

Figure 3 depicts the effect of the heat absorption coefficient on temperature profiles. The inclusion of heat absorption (thermal sink) leads to a reduction in fluid temperature, as evident from the figure where the temperature decreases with increasing ϕ (solid volume fraction). **When the heat absorption coefficient (ϕ) increases, the thermal sink effect in the fluid becomes stronger. This means that a portion of the heat energy generated or transferred within the boundary layer is absorbed or removed by the medium instead of being retained by the fluid.**

The concept of actively designing a system component to absorb heat and reduce the surrounding fluid temperature is the foundation of high-performance cooling.

1. Electronics and Micro-Cooling Systems

- **Heat Sinks and Cooling Plates:** This is the most direct application. In devices like CPUs, GPUs, and power electronics, the fluid (air, water, or a specialized coolant) acts as a medium to transfer heat away. Increasing the effective "heat absorption" capability (like using **nanofluids** with a high solid volume fraction, ϕ) enhances the rate at which heat is pulled from the hot surface, preventing overheating and failure.
  - The material of the cooling component (like fins or microchannels) is engineered to have a high thermal conductivity, effectively functioning as a powerful localized thermal sink to maintain low operating temperatures.

2. High-Temperature Manufacturing Processes

- **Polymer Extrusion and Metal Forming:** In processes like **melt-spinning** (producing polymer fibers) or **hot rolling** (shaping metals), the final product quality is highly dependent on a controlled and rapid cooling rate.
  - The cooling fluid's intrinsic heat absorption capacity (its thermal sink effect) is a critical parameter. A higher ϕ (e.g., in a cooling bath or fluid) means a faster heat removal from the moving surface, allowing for better material properties and reduced manufacturing time.

3. Energy Systems and Aerospace

- **Concentrated Solar Power (CSP) Collectors:** The fluid (often a molten salt or synthetic oil) circulating through the collector needs to absorb solar energy efficiently. Conversely, in the heat exchangers that convert this heat to electricity, the ability of the secondary fluid to act as an effective **thermal sink** (to absorb the heat from the primary fluid) dictates the efficiency of the power cycle.
- **Thermal Protection Systems (TPS) for Hypersonics:** In aerospace vehicles and rocket nozzles exposed to extreme aerodynamic heating, a phenomenon called **transpiration cooling** or using specialized **ablative materials** is employed. These materials or injected coolants absorb massive amounts of heat (acting as a thermal sink) as they change phase or decompose, preventing the structural material from reaching destructive temperatures.

Summary of Engineering Goal

In all these scenarios, the fundamental engineering objective is to **design for a high effective heat absorption coefficient** to ensure the operating temperature of the critical component remains below its maximum allowable limit, thereby improving **performance, longevity, and safety** of the system.

Figure 4 illustrates the impact of the Schmidt number (Sc) on velocity and concentration profiles. An increase in Sc results in a decrease in concentration, which weakens the concentration buoyancy force and consequently lowers the fluid velocity. This decrease in concentration is also accompanied by a thinning of the concentration boundary layer.

1. Chemical and Electrochemical Engineering

- **Mass Transfer Enhancement in Reactors:** A primary goal is to maximize the rate at which a chemical species moves from the bulk fluid to a reactive surface (like a catalyst or an electrode).
  - The mass transfer rate is directly proportional to the concentration gradient at the surface, which is controlled by the thickness of the concentration boundary layer ([4]δ_c).[5] Since δ_c is inversely related to Sc (typically

ISSN 2278-2540 | DOI: 10.51583/IJLTEMAS | Volume XIV, Issue X, October 2025

$\delta_c \propto Sc^{-1/3}$), the high Sc in liquid-phase reactions naturally results in a very thin boundary layer, leading to **high mass transfer coefficients** and faster reaction rates.

- **Electroplating and Corrosion:** In processes like electroplating, the deposition rate is governed by the rate at which metal ions reach the electrode surface. A high Sc (characteristic of the ionic solutions used) ensures a thin diffusion layer, which is essential for uniform, rapid, and controlled deposition.

2. Environmental Engineering and Pollution Control 💧

- **Pollutant Dispersion in Water Bodies:** In modelling how pollutants, salts, or dissolved oxygen spread in lakes, rivers, or oceans, the high Sc of the water dictates that the diffusion of these species is very slow compared to the fluid's momentum spread.
  - Engineers use models based on high Sc to predict that **molecular diffusion is ineffective** at spreading the pollutant, making the process highly dependent on turbulent mixing and convection. This guides the design of outfall diffusers to ensure rapid mixing to prevent "hotspots" of high concentration.

3. Separation Processes 🌡️

- **Membrane Separation (Dialysis/Reverse Osmosis):** The efficiency of a membrane system relies on maintaining a low concentration of the separated species at the membrane surface.
  - The "concentration polarization" layer that builds up near the membrane is essentially the concentration boundary layer. The high Sc of the working liquids means this layer is primarily controlled by the fluid dynamics near the membrane. Engineers design high-shear flow conditions (high velocity, turbulence) to minimize the thickness of this boundary layer, thereby reducing the localized concentration and **improving separation efficiency**.

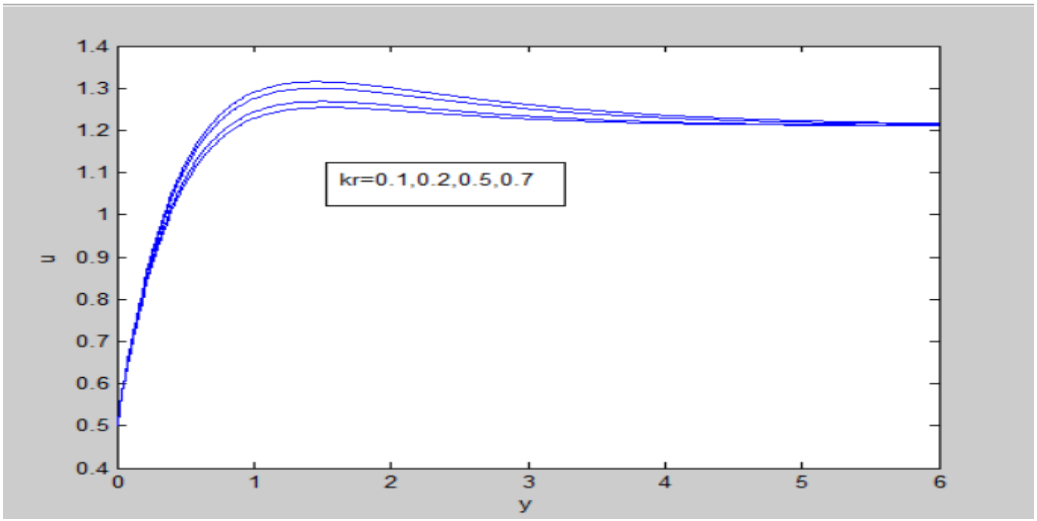

Fig.1 velocity u versus y under the effect of Kr

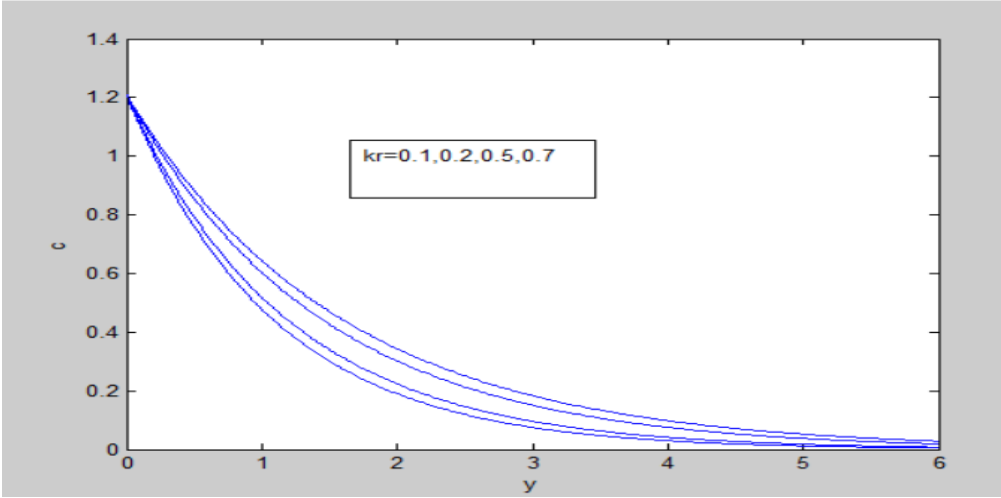

Fig2: Concentration versus y under the effects of Kr.

ISSN 2278-2540 | DOI: 10.51583/IJLTEMAS | Volume XIV, Issue X, October 2025

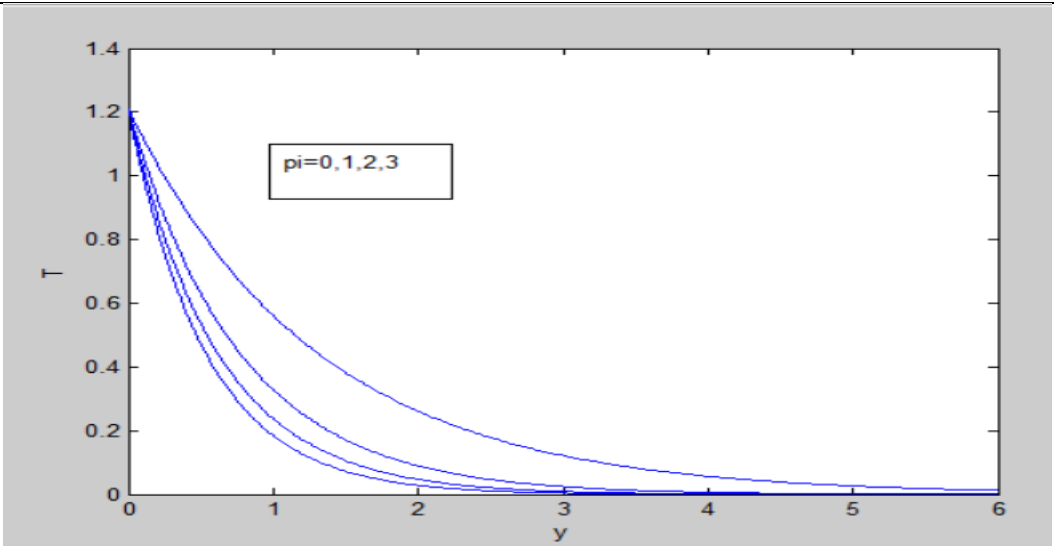

Fig3: Temperature T versus y under the effect of pi(ϕ)

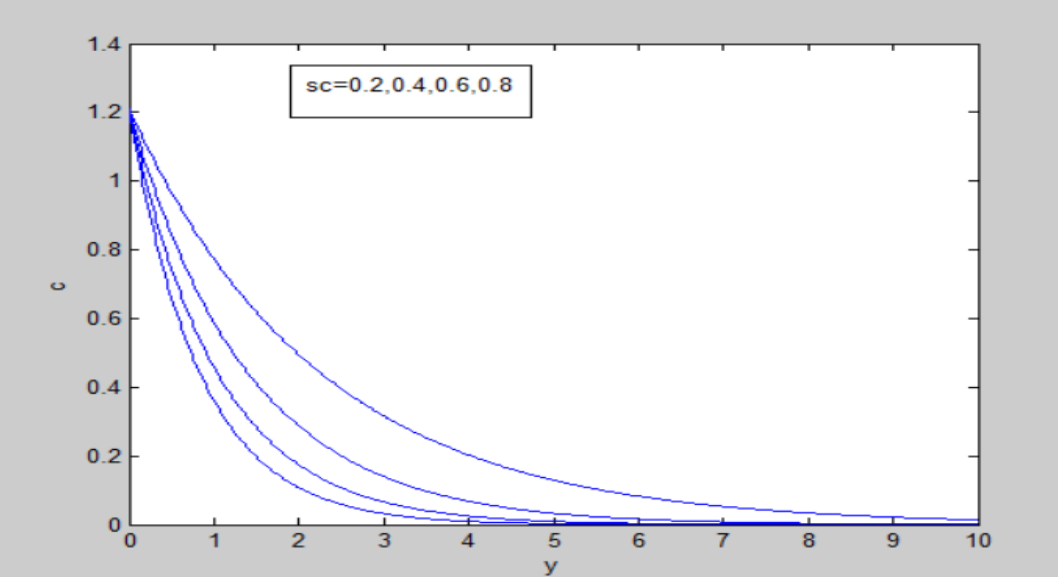

Fig4: Concentration c versus y under the effect of Sc.

III. Conclusion

The plate moved at a constant velocity while the flow was influenced by a transverse magnetic field. The resulting partial differential equations were converted into ordinary differential equations using a two-term series approach and solved in closed form. Numerical calculations of these solutions were performed, and graphical results were generated to show the flow, heat, and mass transfer characteristics, along with their dependence on various physical parameters. It was observed that increasing the chemical reaction parameter led to a reduction in the velocity profiles. Heat absorption effects lowered the fluid temperature, which also caused a decrease in velocity. Additionally, an increase in the Schmidt number reduced the concentration level, further decreasing the fluid velocity. The skin-friction coefficient increased with higher concentration buoyancy effects but decreased with either higher heat absorption coefficient or Schmidt number. Finally, the Nusselt number was found to decrease as the heat absorption coefficient increased.

This study directly connects to real-life applications of magnetohydrodynamics (MHD) in engineering and energy systems. The analysis of flow over a plate under the influence of a transverse magnetic field is important in many industrial and technological processes where electrically conducting fluids, such as liquid metals, plasmas, or ionized gases, are used. For example, in MHD power generation, controlling fluid flow and heat transfer under magnetic fields helps improve energy conversion efficiency. Similarly, in nuclear fusion reactors, magnetic fields are applied to control the motion and temperature of plasma, where heat absorption and chemical reaction parameters influence stability and confinement. In metallurgical applications, such as electromagnetic casting and cooling of molten metals, understanding how parameters like heat absorption and Schmidt number affect velocity, temperature, and concentration profiles helps optimize product quality. The findings also relate to aerospace and space propulsion systems, where MHD effects are used to control plasma flows for thrust generation. Thus, the results of this

ISSN 2278-2540 | DOI: 10.51583/IJLTEMAS | Volume XIV, Issue X, October 2025

research have direct implications for designing efficient MHD-based systems involving heat and mass transfer under magnetic influence.

References

1. Wang, L., Xu, W., Tao, N. and Sun, J., 2025. Free convection heat transfer in thermal imaging processes. International Journal of Thermal Sciences, 215, p.109957.
2. Viswanathan, S.H., Joshi, A., Bartels, L., Sadeghi, K., Vanos, J.K. and Rykaczewski, K., 2025. Impact of human body shape on free convection heat transfer. PloS one, 20(2), p.e0318842.
3. Wang, L., Xu, W., Tao, N. and Sun, J., 2025. Free convection heat transfer in thermal imaging processes. International Journal of Thermal Sciences, 215, p.109957.
   Chamkha, A.J., 2004. Unsteady MHD convective heat and mass transfer past a semi-infinite vertical permeable moving plate with heat absorption. International journal of engineering science, 42(2), pp.217-230.
4. Chamkha, A.J., 1997. Hydromagnetic natural convection from an isothermal inclined surface adjacent to a thermally stratified porous medium. International Journal of Engineering Science, 35(10-11), pp.975-986.
5. Chamkha, A.J., 2004. Unsteady MHD convective heat and mass transfer past a semi-infinite vertical permeable moving plate with heat absorption. International journal of engineering science, 42(2), pp.217-230.
6. Wang, L., Xu, W., Tao, N. and Sun, J., 2025. Free convection heat transfer in thermal imaging processes. International Journal of Thermal Sciences, 215, p.109957.
7. Viswanathan, S.H., Martinez, D.M., Bartels, L., Guddanti, S.S. and Rykaczewski, K., 2023. Impact of human body shape on forced convection heat transfer. International journal of biometeorology, 67(5), pp.865-873.